Preformation probability of light charged particles emitted equatorially in ternary fission of ^{252}Cf

W. M. Seif* and A. S. Hashem
Department of Physics, Faculty of Science, Cairo University, 12613 Giza, Egypt

(Received 24 March 2021; accepted 12 July 2021; published 29 July 2021)

We investigate the preformation probability of the light particle that formed in the preliminary stage of the ternary fission process of the ^{252}Cf nucleus. Considering the equatorial cluster tripartition kinematics, the relative yields of the ternary fission channels with ^{4,6}He, ^{10}Be and ^{14}C as light third nucleus, are calculated. We use the Wentzel-Kramers-Brillouin approximation to calculate the penetrability of the different nuclei involved in the ternary fission process, based on microscopic Skyrme potentials. The obtained results indicate the optimum total excitation energy of the heavy nuclei produced in the α ternary fission channels to be within the range of 3–4 MeV. The estimated α-preformation probability corresponding to this range is comparable with that estimated for the spontaneous α decays of the participating heavy nuclei. While the extracted preformation probability at excitation energy less than its indicated optimum values exhibits unphysical large values, the calculations based on the higher excitation energies indicate extremely small values. In the ternary fission process, the preformation probability of the emitted light particles heavier than the α particle exponentially decreases with increasing its mass number. A phenomenological expression is suggested based on the obtained results to estimate the preformation probability of an emitted cluster of a given mass number.

DOI: 10.1103/PhysRevC.104.014616

I. INTRODUCTION

Besides binary fission, ternary fission has been observed as a probable spontaneous fission mode of heavy nuclei [1,2], where a light third fragment accompanied the two main fission fragments. Ternary nuclear fission rarely appears with a yield of less than 0.1% with respect to binary fission. It has been also detected as induced fission mode. The lightest fragment emits either collinearly or equatorially relative to the heavier fragments. In its equatorial emission, the light particle escapes from a neck connecting the two heavy fission fragments. The mutual Coulomb fields of the fission fragments accelerate the light particle normal to the binary fission axis [3]. In the corresponding collinear emission, the light particle emits in the direction of the fission axis connecting the three fragments [4–8]. While the equatorial configuration was indicated to be the favored configuration for the light accompanying particles such as ^{4}He, ^{10}Be, ^{14}C [9,10], the collinear emission was indicated to be preferred for the heavier outgoing particles such as ^{48}Ca, ^{50}Ca, ^{54}Ti, and ^{60}Cr [1,2,7,11,12]. True ternary fission of heavy and superheavy nuclei into three nuclei of comparable sizes would happen but just collinearly [9].

The cold ternary breakup of ^{252}Cf has been studied using the triple γ coincidence technique where ^{4,6}He, ^{10}Be, and ^{14}C were observed as light third fragments [13–15]. The isotopic yields for the α ternary splitting of ^{252}Cf per 100 fission events has been measured [16,17]. The highest yield has been obtained for the ternary fission channel $^{103}\mathrm{Zr} + {}^{4}\mathrm{He} + {}^{145}\mathrm{Ba}$. The relative ternary yields of ^{5,6}He and ^{10}Be accompanied fission of ^{252}Cf were also measured. α particles were observed as light third particle with the ratio of about 10^{-3} with respect to binary fission events of ^{240,242}Pu, ^{242,244}Cm, ^{250,252}Cf, and ^{256,257}Fm nuclei [18]. Less ratio of about 10^{-4} has been verified for the fissioning $^{243-248}$Cm isotopes [19]. The ^{10}Be nuclei have been observed as emitted light third particle with a relative yield of about 10^{-5}, relative to binary spontaneous fission events [16,20,21]. Ternary fission channels accompanied by other light particles, such as ^{5,7}He [17,22], ^{8}Li, and ^{14}C [13–15] isotopes, were observed with relative yields of about 10^{-4}–10^{-5} in spontaneous fission of ^{252}Cf [19]. Ternary heavier fragments like ^{34}Si have been observed with a probability of about 10^{-10} [21]. An island of considerable yields of the collinear cluster tripartition of ^{252}Cf was reported as true ternary fission with a light charged particle having mass up to $A = 52$ (^{52}Ca) [4,5]. Generally, it was indicated that the relative yield of ternary fission channels decreases upon increasing the mass number of the emitted light particle. Various theoretical studies have been achieved over the past two decades to study the probable spontaneous cluster tripartition of $^{244-260}$Cf [10], ^{260}No [23,24], ^{242,250}Cm [25,26] with possible light nuclei of mass numbers $A = 4$–52.

It has been indicated that the kinetic energy of α particles produced in the ternary fission of ^{252}Cf is mostly showing a Gaussian distribution [22] with an average kinetic energy near 16 MeV and a maximum value larger than 25 MeV. This energy is on average larger than that of the α particles emitted in regular α decays. This results in longer α tracks. That is why the α particles emitted in ternary fission are called "long range alphas". These long range α particles were reported for the first time by Alvarez *et al.* [27]. The average kinetic energy of the other possible ternary particles ^{5,6,7}He, ^{8}Li, ^{10}Be, and ^{14}C changes within the range of 8–26 MeV [15,21,28]. The spontaneous ternary breakup of heavy and superheavy nuclei

*wseif@sci.cu.edu.eg

as a rule frees large amounts of energy. This liberated energy essentially appears as kinetic and excitation energy of the produced fragments, and partly give rise to γ ray and/or neutron emissions [29]. The Q value of the reaction shares between the total kinetic and excitation energies of the three resulting fragments. The total excitation energy is often smaller in ternary than in binary break up [30]. The emission of a third particle with a kinetic energy then takes place at the cost of the total excitation energy of the ternary system [31].

In its direct mechanism, ternary splitting takes place as a synchronous decay where the three fragments are simultaneously detected. In this scenario, few shared nucleons are clustered as a recognizable third particle in the neck region between two heavy entities in the fissioning nucleus [32]. Collinear cluster tripartition (CCT) with ternary particles of masses $A > 30$ and high yields of about 0.5% per fission have been observed from the spontaneous fission ^{252}Cf and the neutron induced fission of ^{235}U [5]. In these cases, the CCT was viewed as a successive decay, with three fragments being conceived from successive binary splitting. In its two-step scenario, a dinuclear system is formed in the fissioning nucleus and then the third particle is clustered inside the lighter formed nucleus. Then, the three fragments are collinearly emitted. The kinematics of the produced fragments in CCT assuming a two-stage splitting procedure has been considered [33,34]. The kinetic energies of such fission fragments can be systematically deduced from momentum and energy conservation. It was expected that the trifragmentation occurs in two successive stages from super- and hyperdeformed states of nuclei [35]. At the initial stage, a first neck rupture of the parent nucleus (A) takes place, forming two fragments (A_1 and A_{CN23}). Often, the first heavy nucleus A_1 is of a neutron and/or a proton closed shell. In the next stage, the nucleus A_{CN23} splits into a second heavy nucleus (A_2) and light third nucleus (A_3). The fission axes at which the two successive fragmentation processes occur are perfectly collinear. In general, the kinematics of the three nuclei participating in the ternary fission process depends on several parameters. Namely, it depends on the mechanism of the process, either it is direct or sequential, collinear or equatorial, and the positions of the formed nuclei relative to each other, as well as the excitation energy of the three formed nuclei and that of the intermediate nucleus.

In the present work, we will consider the kinematics of equatorial configuration to calculate the relative yields of the various ternary fission channels of ^{252}Cf with ^{4,6}He, ^{10}Be, and ^{14}C as light third fragments. The excitation energies of the fragments will be taken into account. We will study the optimum values of the excitation energies and the estimated preformation probability of the light charged particle in ternary fission. In the next section, we outline the general theoretical framework of ternary fission kinematics. The numerical results are presented and discussed in Sec. III. Finally, the conclusion is given in Sec. IV.

II. THEORETICAL FRAMEWORK

The equatorial (orthogonal) ternary fission probably proceeds as follows, Fig. 1. The parent nucleus deforms in shape into the binary system of the two heavy nuclei A_1 and $A_{CN23}(A_2 + A_3)$, at the scission configuration. Immediately before scission, the light emitted particle might be distinguishably formed on the surface of the intermediate nucleus A_{CN23}, within the neck region joining A_1 and A_{CN23}. Then, A_3 emits in a direction perpendicular to the fission axis, as a result of the high Coulomb force [36].

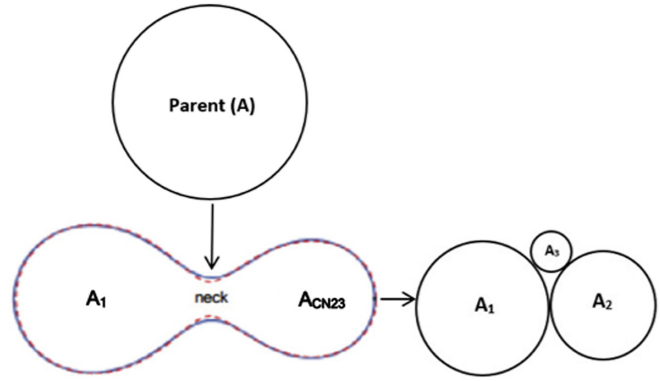

FIG. 1. A scheme of ternary fission of a parent nucleus in two-step process, where the light nucleus (A_3) is formed between the two heavy fragments A_1 and A_2 perpendicular to the fission axis in equatorial configuration [36].

Generally, the conservation of energy in the preliminary stage gives

$$Q_{1CN23} + E^*_A = KE_1 + E^*_{A_1} + KE_{CN23} + E^*_{A_{CN23}}.$$

Here, Q_{1CN23} is the Q value of the preliminary stage, while E^*_A, $E^*_{A_1}$, and $E^*_{A_{CN23}}$ are the excitation energies of the parent nucleus (A), heavy fragment (A_1), and the intermediate nucleus (A_{CN23}), respectively. KE_1 and KE_{CN23} are the kinetic energies of the heavy fragment (A_1) and the intermediate nucleus (A_{CN23}), respectively.

While the parent nucleus spontaneously decays ($E^*_A = 0$ MeV), the effective released energy $Q_{\text{eff}12}$ can be defined in terms of the excitation energies of the two heavy nuclei ($E^*_I = E^*_{A_1} + E^*_{A_{CN23}}$) and its value in terms of the ground state masses of the involved nuclei (Q_{1CN23}) as

$$Q_{\text{eff}12} = Q_{1CN23} - E^*_I. \tag{1}$$

The conservation of energy in the posterior stage yields

$$Q_{23} + E^*_{II} + KE_{CN23} = KE_2 + KE_3.$$

Here, Q_{23} and E^*_{II} represent the Q value and excitation energy in stage (II), respectively. KE_2 and KE_3 are the kinetic energies of the medium heavy fragment (A_2) and light nucleus (A_3), respectively,

$$E^*_{II} = E^*_{CN23} - E^*_{A_2} - E^*_{A_3}.$$

The released energy in ternary fission (Q_{TF}) can be obtained in terms of the masses of the involved nuclei or in terms of their total kinetic (TKE $= \sum_i KE_i$) and excitation (TXE $= \sum_i E^*_{A_i}$) energies, The excitation energy of the intermediate nucleus totally contributes to the kinetic and excitation energies of $A_{2,3}$,

$$Q_{TF} = \text{TKE} + \text{TXE}. \tag{2}$$

To estimate the relative yield of each probable fragmentation channel and then the total yield, one needs to calculate accurately the interaction potentials between the fragments participating in each stage, A_1 and A_{CN23} in the preliminary stage, and between A_1, A_2, and A_3 in stage II. These potentials are of importance for determining the penetration probability in each stage. Here, we will use the Hamiltonian energy density approach based on the Skyrme energy density functional [37,38] in terms of the Skyrme-SLy4 [39] parametrization of the NN interaction, and the proton-proton interaction, to calculate the nuclear V_N and Coulomb V_C parts of the interaction potential,

$$V_N(R) + V_C(R) = E_{\rm tot}(R) - E_1 - E_2. \tag{3}$$

While R represents the distance between the centers of mass of the interacting nuclei, $E_{\rm tot}(R)$ is the total energy of the interacting nuclear system, and $E_{1,2}$ are the binding energies of the two interacting nuclei,

$$\begin{aligned} E_{\rm tot}(R) &= \int H[\rho_{1p}(\vec{r}) + \rho_{2p}(\vec{r}-\vec{R}),\, \rho_{1n}(\vec{r}) + \rho_{2n}(\vec{r}-\vec{R})]d\vec{r}, \\ E_1 &= \int H[\rho_{1p}(\vec{r}),\, \rho_{1n}(\vec{r})]d\vec{r}, \\ E_2 &= \int H[\rho_{2p}(\vec{r}),\, \rho_{2n}(\vec{r})]d\vec{r}. \end{aligned} \tag{4}$$

The energy density functional H includes the kinetic, nuclear (sky), and Coulomb (coul) parts,

$$H = \frac{\hbar^2}{2m}[\tau_p(\vec{r}) + \tau_n(\vec{r})] + H_{\rm sky}(\vec{r}) + H_{\rm coul}(\vec{r}). \tag{5}$$

The kinetic energy densities τ_i $(i = p, n)$ for protons and neutrons are given by

$$\begin{aligned} \tau_i(\vec{r}) = {} & \frac{3}{5}(3\pi^2)^{2/3}\rho_i^{5/3} + \frac{1}{36}\frac{(\vec{\nabla}\rho_i)^2}{\rho_i} + \frac{1}{3}\Delta\rho_i \\ & + \frac{1}{6}\frac{\vec{\nabla}\rho_i\vec{\nabla}f_i + \rho_i\Delta f_i}{f_i} - \frac{1}{12}\rho_i\left(\frac{\vec{\nabla}f_i}{f_i}\right)^2 \\ & + \frac{1}{2}\rho_i\left(\frac{2m}{\hbar^2}\frac{W_0}{2}\frac{\vec{\nabla}(\rho+\rho_i)}{f_i}\right)^2. \end{aligned} \tag{6}$$

Here, $\rho_{i=p,n}$ denote the proton and neutron densities of the nucleus. The total density ρ is their sum. W_0 defines the strength of the Skyrme spin-orbit interaction. The effective-mass form factor f_i is given by [40]

$$f_i(\vec{r}) = 1 + \frac{2m}{\hbar^2}\left\{\begin{array}{l} \frac{1}{4}\left[t_1\left(1+\frac{x_1}{2}\right) + t_2\left(1+\frac{x_2}{2}\right)\right]\rho(\vec{r}) \\ +\frac{1}{4}\left[t_2\left(x_2+\frac{1}{2}\right) - t_1\left(x_1+\frac{1}{2}\right)\right]\rho_i(\vec{r}) \end{array}\right\}. \tag{7}$$

The nuclear energy density part reads

$$\begin{aligned} H_{\rm sky}(\vec{r}) = {} & \frac{t_0}{2}\left[\left(1+\frac{x_0}{2}\right)\rho^2 - \left(x_0+\frac{1}{2}\right)\left(\rho_p^2+\rho_n^2\right)\right] + \frac{1}{12}t_3\rho^\alpha\left[\left(1+\frac{x_3}{2}\right)\rho^2 - \left(x_3+\frac{1}{2}\right)\left(\rho_p^2+\rho_n^2\right)\right] \\ & + \frac{1}{4}\left[t_1\left(1+\frac{x_1}{2}\right) + t_2\left(1+\frac{x_2}{2}\right)\right]\tau\rho + \frac{1}{4}\left[t_2\left(x_2+\frac{1}{2}\right) - t_1\left(x_1+\frac{1}{2}\right)\right](\tau_p\rho_p + \tau_n\rho_n) \\ & + \frac{1}{16}\left[3t_1\left(1+\frac{x_1}{2}\right) - t_2\left(1+\frac{x_2}{2}\right)\right](\vec{\nabla}\rho)^2 - \frac{1}{16}\left[3t_1\left(x_1+\frac{1}{2}\right) + t_2\left(x_2+\frac{1}{2}\right)\right][(\vec{\nabla}\rho_n)^2 + (\vec{\nabla}\rho_p)^2] \\ & - \frac{W_0^2}{4}\frac{2m}{\hbar^2}\left[\frac{\rho_p}{f_p}(2\vec{\nabla}\rho_p + \vec{\nabla}\rho_n)^2 + \frac{\rho_n}{f_n}(2\vec{\nabla}\rho_n + \vec{\nabla}\rho_p)^2\right]. \end{aligned} \tag{8}$$

The different terms in this expression consider the zero- and finite-range, density dependent, effective-mass, and spin-orbit, as well as tensor coupling with spin and gradient contributions [37,41]. The Skyrme-SLy4 parametrization [39] of the $t_{i=0-3}$, $x_{i=0-3}$, and α parameters of the NN Skyrme nuclear interaction will be used in the present calculations. The direct and exchange parts of the Coulomb energy density read

$$H_{\rm coul}(\vec{r}) = \frac{e^2}{2}\rho_p(\vec{r})\int\frac{\rho_p(\vec{r'})}{|\vec{r}-\vec{r'}|}d\vec{r'} - \frac{3e^2}{4}\left(\frac{3}{\pi}\right)^{1/3}(\rho_p(\vec{r}))^{4/3}. \tag{9}$$

In this expression, the Slater approximation [42,43] is used to represent the exchange second term. The neutron and proton density distributions of a given nucleus (A, Z, N) will be used in the spherical symmetric Fermi form

$$\rho_i(\vec{r}) = \frac{\rho_{0i}}{1+\exp\left(\frac{r-R_{0i}}{a_i}\right)}, \quad i = \{n,\ p\}. \tag{10}$$

The half-density radius R_{0i} and diffuseness a_i parameters are parametrized as [44]

$$\begin{aligned} R_{0n}({\rm fm}) &= 0.953(N)^{\frac{1}{3}} + 0.015(Z) + 0.774, \\ R_{0p}({\rm fm}) &= 1.322(Z)^{\frac{1}{3}} + 0.007(N) + 0.022, \\ a_n({\rm fm}) &= 0.446 + 0.072(N/Z), \\ a_p({\rm fm}) &= 0.449 + 0.071(Z/N). \end{aligned} \tag{11}$$

The densities are normalized through the ρ_{0i} parameter to conserve the neutron (N) and proton (Z) numbers of the nucleus. More details regarding the method of calculating the potential based on the Skyrme nucleon-nucleon interaction can be found in Refs. [45–47]. The total interaction potential is then taken as the sum of its nuclear, Coulomb, and centrifugal parts,

$$V(r) = \lambda\, V_N(r) + V_C(r) + V_\ell(r). \tag{12}$$

TABLE I. α-preformation probability S_α [Eq. (17)] for the observed α ternary fission channels of ^{252}Cf, extracted from comparing the experimental relative yield ($Y_{\rm exp}$) with that calculated ($Y_{\rm cal}$) at excitation energy of stage (I) $E_I^*(E_{A_1}^*, E_{A_{CN23}}^*) = 3$ MeV and 4 MeV, considering equatorial ($KE_\alpha = 15.7$ MeV) configuration of the ternary system.

		$E_I^*(E_{A_1}^*, E_{A_{CN23}}^*) = 3$ MeV		$E_I^*(E_{A_1}^*, E_{A_{CN23}}^*) = 4$ MeV	
Ternary fission channel	Experimental yield ($Y_{\rm exp}$ [13–16])	$Y_{\rm cal}$	$S_\alpha = Y_{\rm cal}({\rm without}\ S_\alpha)/Y_{\rm exp}$	$Y_{\rm cal}$	$S_\alpha = Y_{\rm cal}({\rm without}\ S_\alpha)/Y_{\rm exp}$
^{156}Nd + ^{92}Kr + ^{4}He	2.00×10^{-3}	1.85×10^{-4}	9.26×10^{-2}	2.33×10^{-5}	1.16×10^{-2}
^{152}Ce + ^{96}Sr + ^{4}He	8.00×10^{-3}	1.86×10^{-4}	2.32×10^{-2}	2.34×10^{-5}	2.93×10^{-3}
^{150}Ce + ^{98}Sr + ^{4}He	1.40×10^{-2}	5.52×10^{-4}	3.94×10^{-2}	6.86×10^{-5}	4.90×10^{-3}
^{149}Ce + ^{99}Sr + ^{4}He	1.80×10^{-2}	4.91×10^{-4}	2.73×10^{-2}	5.84×10^{-5}	3.24×10^{-3}
^{148}Ce + ^{100}Sr + ^{4}He	2.10×10^{-2}	1.87×10^{-4}	8.90×10^{-3}	2.29×10^{-5}	1.09×10^{-3}
^{148}Ba + ^{100}Zr + ^{4}He	3.80×10^{-2}	3.09×10^{-4}	8.12×10^{-3}	3.75×10^{-5}	9.88×10^{-4}
^{147}Ce + ^{101}Sr + ^{4}He	1.40×10^{-2}	1.60×10^{-4}	1.14×10^{-2}	1.85×10^{-5}	1.32×10^{-3}
^{147}Ba + ^{101}Zr + ^{4}He	8.20×10^{-2}	3.05×10^{-4}	3.71×10^{-3}	3.67×10^{-5}	4.48×10^{-4}
^{146}Ba + ^{102}Zr + ^{4}He	9.00×10^{-3}	3.81×10^{-4}	4.23×10^{-2}	4.92×10^{-5}	5.47×10^{-3}
^{145}Ba + ^{103}Zr + ^{4}He	8.40×10^{-2}	3.60×10^{-4}	4.29×10^{-3}	4.56×10^{-5}	5.43×10^{-4}
^{144}Ba + ^{104}Zr + ^{4}He	1.70×10^{-2}	4.21×10^{-4}	2.48×10^{-2}	5.59×10^{-5}	3.29×10^{-3}
^{142}Xe + ^{106}Mo + ^{4}He	1.80×10^{-2}	2.89×10^{-4}	1.61×10^{-2}	3.91×10^{-5}	2.17×10^{-3}
^{141}Xe + ^{107}Mo + ^{4}He	3.00×10^{-2}	2.86×10^{-4}	9.54×10^{-3}	3.84×10^{-5}	1.28×10^{-3}
^{140}Xe + ^{108}Mo + ^{4}He	7.00×10^{-3}	3.54×10^{-4}	5.06×10^{-2}	5.09×10^{-5}	7.28×10^{-3}
^{136}Te + ^{112}Ru + ^{4}He	1.10×10^{-2}	6.80×10^{-4}	6.18×10^{-2}	1.05×10^{-4}	9.59×10^{-3}
^{132}Sn + ^{116}Pd + ^{4}He	6.00×10^{-3}	4.55×10^{-4}	7.58×10^{-2}	7.75×10^{-5}	1.29×10^{-2}

The radial dependence of the centrifugal part of the potential is considered in its ordinary form, $V_\ell(r) = \ell(\ell+1)\hbar^2/2\mu r^2$ [48]. The Bohr-Sommerfeld quantization condition [49,50] can be used to normalize the nuclear part of the potential, through the parameter λ, to guarantee the quasi-bound state of the binary system before fragmentation, in each stage,

$$\int_{R_1}^{R_2} k(r)d\vec{r} = (2n+1)\frac{\pi}{2}. \tag{13}$$

Here, $k(r) = \sqrt{2\mu|V(r)-Q|/\hbar^2}$, μ is the reduced mass of the two nuclei involved in each stage, and Q is the corresponding effective Q value. The quantum number n corresponding to the value of λ closest to unity will be considered. Now, the penetration probability for the two heaviest nuclei A_1 and A_2 can be calculated using the semiclassical Wentzel-Kramers-Brillouin (WKB) approximation [51,52] as

$$P_{12} = \exp\left[-\frac{2}{\hbar}\int_{R_{2(12)}}^{R_{3(12)}}\sqrt{2\mu_{1CN23}|V_{1CN23}(r)-Q_{\rm eff12}|}dr\right] \tag{14}$$

and

$$P_{i=23,13} = \exp\left[-\frac{2}{\hbar}\int_{R_{2i}}^{R_{3i}}\sqrt{2\mu_i|V_i(r)-KE_{3\,\rm exp}|}dr\right] \tag{15}$$

respectively. V_{1CN23} defines the total interaction potential between the heaviest fragment A_1 and the intermediate nucleus A_{CN23}. $V_{23}(V_{13})$ defines the potential between the light emitted nucleus and the medium A_2 (heaviest A_1) fragment. $KE_{3\,\rm exp}$ is the experimental kinetic energy of A_3. In the equatorial (orthogonal) configuration, there are three different barriers and the light particle is formed in the neck region between A_1 and A_{CN23} before its emission perpendicular to their fission axis as a result of the repulsive Coulomb force. $R_{2i,3i(i=12,\,13,\,23)}$ are the second and third classical turning points, defined separately for each total interaction potential, at which the corresponding potential equals the released energy, $Q_{\rm eff12}$ or $KE_{3\,\rm exp}$ in stage II. The relative yield of a given ternary fission channel ($A_{1,2,3}$) can be calculated in terms of the total penetration probability of equatorial ternary fission ($P_{TF} = P_{12} \times P_{23} \times P_{13}$ [12]), and the penetration probability of the corresponding binary fission of the parent nucleus P_{BF} as

$$Y_{\rm cal} = \frac{S_3 \times P_{TF}}{P_{BF}}. \tag{16}$$

Here, S_3 represents the preformation probability of the emitted light nucleus A_3 in the preliminary stage of the ternary fission process. P_{BF} is the penetrability of the corresponding quasi-binary-fission probability yielding A_1 and $A_{CN23}(A_2 + A_3)$. The preformation probability S_3 (A_3) can be then estimated by comparing the calculated yield without considering S_3 [$Y_{\rm cal}({\rm without}\ S_3)$] with the experimental yield ($Y_{\rm exp}$) [1,2,13–16,20],

$$S_3 = \frac{Y_{\rm cal}({\rm without}\ S_3)}{Y_{\rm exp}}. \tag{17}$$

III. RESULTS AND DISCUSSION

In the present work, we investigate the kinematics of the equatorial tripartition of the spontaneously fissioning ^{252}Cf nucleus, as two-step process where the light emitted particle is preformed inside the fissioning nucleus in the first step. In the framework of the energy density formalism based on the Skyrme-SLy4 parametrization of the NN force, we calculated the interaction potential between the two heavy fragments (V_{12}) and that between them and the light emitted particle (V_{13} and V_{23}). The partial yields of the experimentally observed channels of ternary fission, relative to the

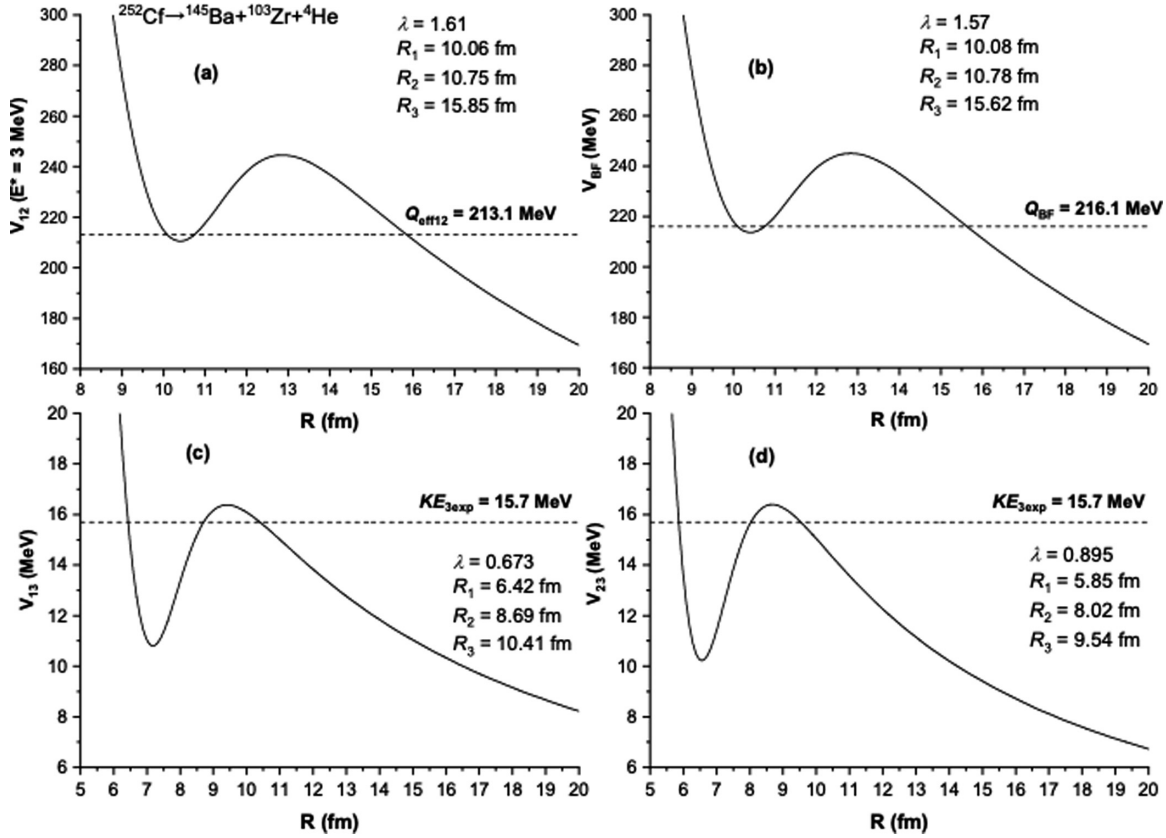

FIG. 2. The radial dependence of the mutual interaction potentials (a) V_{12} (^{145}Ba, ^{103}Zr), (b) V_{BF} (^{145}Ba, ^{107}Mo), (c) V_{13} (^{145}Ba, ^{4}He), and (d) V_{23} (^{103}Zr, ^{4}He) which are involved in the ternary fission channel ^{252}Cf ($A_1 = {}^{145}$Ba, $A_2 = {}^{103}$Zr, $A_3 = {}^{4}$He), based on the Skyrme-SLy4 nucleon-nucleon interaction. The turning points ($R_{1,2,3}$) corresponding to each binary system and the normalization factor λ [Eq. (12)] obtained from the Bohr-Sommerfeld quantization condition are given in each panel. The centrifugal potential of the α particle (^{4}He) with the minimum angular momentum quantum number giving three turning points is considered.

corresponding binary fission, are then calculated based on the penetration probabilities of the fragments involved in each stage. The influence of the excitation energies of the nuclei involved in the ternary fission process on the preformation probability of the emitted light cluster is studied, to obtain information on the estimated preformation probability at the optimum values of the excitation energies. We focus on the observed channels of the ternary fission modes of ^{252}Cf that include ^{4,6}He, ^{10}Be, and ^{14}C clusters as emitted light particles [1,2,13–16,20].

Table I shows the calculated partial yields of the different observed channels of ^{252}Cf ternary fission (column 1) with the α particle (^{4}He) being the emitted light particle. The relative yields observed for the presented 16 channels, per 100 fission events, are listed in the second column of Table I. As seen in Table I for the ^{4}He ternary fission channels of ^{252}Cf, while the mass number of the heaviest fragment is ranged between $A_1 = 132$ (^{132}Sn) and $A_1 = 156$ (^{156}Nd), the mass number of the corresponding second heavy fragment is ranged between $A_2 = 116$ (^{116}Pd) and $A_2 = 92$ (^{92}Kr). The maximum relative yields are obtained for the ternary channels of ($A_1 = {}^{145}$Ba, $A_2 = {}^{103}$Zr, $A_3 = {}^{4}$He, $Y_{\rm exp} = 0.084\%$) and (^{147}Ba, ^{101}Zr, ^{4}He; 0.082%). The total relative yield for the ^{4}He channels is about 0.379%. All the available experimental data on ternary fission such as the relative yield and the kinetic energy represent average values, and their maximum values are mostly related to equatorial emission. The relative yields calculated with excitation energy of prior stage (I) $E_I^* = 3$ MeV, corresponding to $E_{A_1}^* = 1.5$ MeV and $E_{A_{CN23}}^* = 1.5$ MeV, and $E_I^* = 4$ MeV, corresponding to $E_{A_1}^* = 2$ MeV and $E_{A_{CN23}}^* = 2$ MeV, for the equatorial tripartition configuration are listed in columns 3 and 5, respectively. The experimental value of the kinetic energy of the emitted light cluster ($KE_{3\,\rm exp}$) is used in calculating its penetration probabilities P_{13} and P_{23} [1,2,13–16,20]. The kinetic energy of the emitted α particles show a Gaussian distribution centered at 15.7 MeV, at which the yield reaches its maximum value. An example for the total mutual interaction potentials between the participating nuclei is shown in Fig. 2 for the ^{252}Cf ($A_1 = {}^{145}$Ba, $A_2 = {}^{103}$Zr, $A_3 = {}^{4}$He) ternary fission channel.

The estimated preformation probability of α particles for the tabulated channels, as extracted by comparing the calculated yields $Y_{\rm cal}(E_I^* = 3$ MeV) and $Y_{\rm cal}(E_I^* = 4$ MeV) with the experimental values are listed in columns 4 and 6 of Table I, respectively. The values of S_α based on $E_I^* = 4$ MeV lie between 0.001 and 0.013 with an average value of 0.004. The preformation probability of α particle that extracted from the calculations based on $E_I^* = 3$ MeV ranges

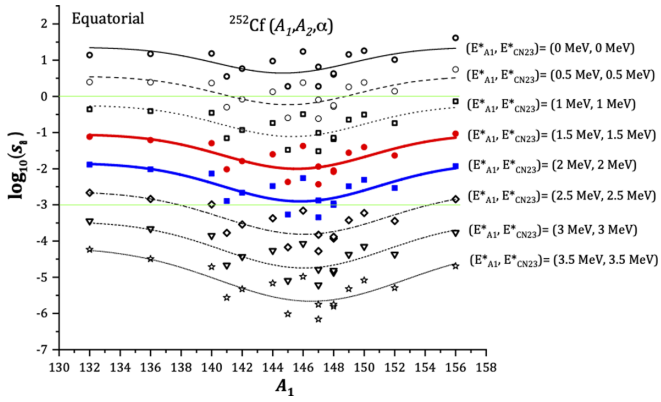

FIG. 3. Logarithms of the α preformation probability versus the heaviest fragment mass number (A_1) for the equatorially observed α ternary fission channels of ^{252}Cf, as extracted from the experimental relative yield and its values calculated at various excitation energy of stage (I) $E_I^*(E_{A_1}^*, E_{A_{CN23}}^*) = 0$–7 MeV with $KE_\alpha = 15.7$ MeV. Continuous curves and the lines corresponding to $\log_{10}(S_\alpha) = 0$ and -3 (green lines) are drawn to guide the eye.

between $S_\alpha = 0.004$ and $S_\alpha = 0.093$, with an average value of about 0.031.

We display in Fig. 3 the decimal logarithm of the extracted S_α based on the equatorial calculations of the relative yields, considering the excitation energy of prior stage (I) $E_I^*(E_{A_1}^*, E_{A_{CN23}}^*)$ within the range from zero to 7 MeV, where E_I^* is distributed equally between A_1 and A_{CN23}, versus the mass number of the fragment A_1 participating in the different channels listed in Table I. The solid, dashed, and dotted curves are drawn to guide the eye for the extracted values of S_α corresponding to the different considered values of the excitation energy E_I^*. The two green horizontal lines corresponding to $\log_{10}(S_\alpha) = 0$ and -3 are also drawn in Fig. 3 to guide the eye to the unphysical values of $S_\alpha > 1$ and to its extreme low values smaller than 10^{-3}. Figure 3 shows that increasing the excitation value E_I^* decreases the estimated preformation probability, due to decreasing the calculated relative yield. The calculations based on $E_I^* = 0$–1 MeV lead to unphysical large values of $S_\alpha > 1$. $E_I^* = 2$ MeV yields large values of S_α approaching unity. However, the calculations based on $E_I^* = 3$–4 MeV yields estimated S_α within the range indicated for the nuclei in the neighborhood of the participating heavy nuclei. This indicates that the optimum excitation energy of stage (I) for the channels including α particle as emitted light particle is ranging between 3 and 4 MeV. Considering $E_I^* \geqslant 5$ MeV leads to extremely small values of $S_\alpha < 10^{-4}$. The highest known excitation state of the A_1 nuclei participating in the investigated channels ranges between 2.304 MeV [^{148}Ba($J^\pi = 12^+$)] and 7.244 MeV [^{132}Sn($J^\pi = 7^-$)] [53].

The preformation of A_3 within the surface region of the parent nucleus is frequently followed by its emission as α or cluster decay process. An example related to the present case is the α-decay mode of ^{252}Cf, which produces the ^{248}Cm daughter nucleus with a branching ratio of 96.9% [54]. Therefore, the emitted cluster in the ternary fission process is often formed simultaneously with a preliminary quasifission stage. The Q value of the quasifission process producing the binary $A_1 + A_{CN23}(A_2, A_3)$ system in the observed ternary fission channels of ^{252}Cf is usually greater than that yielding the binary $A_2 + A_{CN13}(A_1, A_3)$ system. For instance, for the ^{108}Mo + ^{4}He + ^{140}Xe, ^{108}Mo + ^{6}He + ^{138}Xe, ^{108}Mo + ^{10}Be + ^{134}Te, ^{108}Mo + ^{14}C + ^{130}Sn channels, with the ^{108}Mo nucleus appearing as a second heavy nucleus, the $Q(A_1, A_{CN23})$ values are about 225 MeV, 226 MeV, 234 MeV, and 237 MeV, respectively. The corresponding smaller $Q(A_2, A_{CN13})$ value is about 219 MeV. Also, for the ^{108}Mo + ^{4}He + ^{140}Xe, ^{108}Mo + ^{6}He + ^{138}Xe, ^{108}Mo + ^{10}Be + ^{134}Te, ^{108}Mo + ^{14}C + ^{130}Sn channels, which have the ^{140}Xe nucleus as a common heaviest nucleus, the $Q(A_1, A_{CN23})$ value is about 225, while the corresponding smaller $Q(A_2, A_{CN13})$ values are about 219 MeV, 217 MeV, 212 MeV, and 208 MeV, respectively. This supports the scenario that the emitted light cluster is formed within the surface region of the A_{CN23} ($A_2 + A_3$) composite system. Because the nucleons in the overlapped-density (neck) region between the two preliminary fissioning nuclei are of the less binding energy and the maximum single-particle excitation energy above the Fermi energy level of the nucleus, the preferred position of the formed A_3 nucleus lies in this region.

The first particle heavier than ^{4}He that is observed as emitted third particle in ternary fission of ^{252}Cf is the ^{6}He nucleus. 15 ternary fission channels of ^{252}Cf were observed with ^{6}He being the light third nucleus. These channels and their relative yields are respectively listed in the first and second columns of Table II. The mass number of the heaviest produced fragment observed in the ^{6}He ternary fission of ^{252}Cf ranges between $A_1 = 130$ (^{130}Sn) and 156 (^{156}Nd), while the mass number of the corresponding second heavy fragment ranges between $A_2 = 116$ (^{116}Pd) and 90 (^{90}Kr). The four ^{90}Kr, ^{104}Mo, ^{110}Ru, and ^{114}Pd appeared in the ^{6}He channels as A_1 fragment, but were not observed in the ^{4}He channels. The maximum relative yields were obtained for the ternary channels of (^{138}Xe, ^{108}Mo, ^{6}He, $Y_{\rm exp} = 0.03\%$) and (^{150}Ce, ^{96}Sr, ^{6}He; 0.021%). The total relative yield for the ^{6}He channels is about 0.163%. The observed yield reaches its maximum value at ^{6}He kinetic energy of about 12.3 MeV. Figure 4 shows the decimal logarithm of the ^{6}He preformation probability ($S_{^6\rm He}$), as extracted by comparing the calculated relative yields at $E_I^* = 1$–7 MeV with the experimental values, for the ^{6}He ternary fission channels of ^{252}Cf. The fit lines for the calculated preformation probability as a function of A_1 are drawn in Fig. 4 to guide the eye. As shown in Fig. 4, increasing the excitation value $E_I^*(E_{A_1}^*, E_{A_{CN23}}^*)$ decreases the estimated value of the preformation probability. The calculations based on $E_I^* = 1$ MeV yields an average large values of $S_{^6He}$ of the order of 10^{-2}. Increasing the value of the excitation energy of stage (I) to $E_I^* = 2$, 3, and 4 MeV decreases the order of magnitude of the estimated average value of ($S_{^6\rm He}$) to be of about 10^{-3}, 10^{-4}, and 10^{-5}, respectively. The highest known excitation energy of the A_1 nuclei involved in the investigated channels of ^{6}He ranges from 2.737 MeV [^{156}Nd(16^+)] to 7.566 MeV [^{134}Te(15^+)]. The average relative yields that calculated at excitation energy $E_I^*(E_{A_1}^*, E_{A_{CN23}}^*) = 3$ and 4 MeV and the corresponding preformation probabilities of ^{6}He as extracted from the calculated and the experimental relatives

TABLE II. The average relative yield $Y_{\rm cal}^{\rm ave}$ (in column 3) and the estimated average preformation probability $S_c^{\rm ave}$ (in column 4) considering the optimum excitation energy $E_I^*(E_{A_1}^*, E_{A_{CN23}}^*) = 3$ and 4 MeV, for the observed ^{6}He, ^{10}Be, and ^{14}C ternary fission channels of ^{252}Cf (in column 1). Also listed are the experimental relative yields (column 2), the preformation probability estimated by the phenomenological formula given by Eq. (18) (column 5), and the standard deviation between $S_c^{\rm ave}$ and S_c [Eq. (18)].

Ternary fission channel	Experimental yield ($Y_{\rm exp}$ [13–15,21,28])	$Y_{\rm cal}^{\rm ave}$ ($E_I^* = 3$–4 MeV)	$S_c^{\rm ave}$Eq. (17) ($E_I^* = 3$–4 MeV)	S_c Eq. (18)	Standard Deviation
^{156}Nd + ^{90}Kr + ^{6}He	8.00×10^{-3}	7.53×10^{-6}	4.70×10^{-4}	3.11×10^{-6}	1.553
^{154}Nd + ^{92}Kr + ^{6}He	3.60×10^{-3}	7.35×10^{-6}	1.79×10^{-3}		
^{150}Ce + ^{96}Sr + ^{6}He	2.10×10^{-2}	4.38×10^{-6}	4.51×10^{-4}		
^{148}Ce + ^{98}Sr + ^{6}He	4.90×10^{-3}	3.55×10^{-6}	9.35×10^{-4}		
^{146}Ce + ^{100}Sr + ^{6}He	5.30×10^{-4}	1.19×10^{-6}	3.96×10^{-5}		
^{146}Ba + ^{100}Zr + ^{6}He	1.00×10^{-2}	1.07×10^{-6}	5.65×10^{-5}		
^{144}Ba + ^{102}Zr + ^{6}He	1.30×10^{-2}	8.71×10^{-7}	6.22×10^{-5}		
^{142}Ba + ^{104}Zr + ^{6}He	5.30×10^{-3}	2.75×10^{-7}	5.20×10^{-5}		
^{142}Xe + ^{104}Mo + ^{6}He	1.40×10^{-2}	2.75×10^{-7}	2.11×10^{-5}		
^{140}Xe + ^{106}Mo + ^{6}He	1.90×10^{-2}	2.47×10^{-7}	2.47×10^{-5}		
^{138}Xe + ^{108}Mo + ^{6}He	3.00×10^{-2}	5.35×10^{-8}	1.01×10^{-4}		
^{136}Te + ^{110}Ru + ^{6}He	3.80×10^{-3}	5.99×10^{-8}	1.22×10^{-5}		
^{134}Te + ^{112}Ru + ^{6}He	9.70×10^{-3}	6.00×10^{-8}	2.86×10^{-6}		
^{132}Sn + ^{114}Pd + ^{6}He	4.10×10^{-3}	4.43×10^{-8}	1.23×10^{-5}		
^{130}Sn + ^{116}Pd + ^{6}He	1.60×10^{-2}	4.70×10^{-8}	5.87×10^{-6}		
^{146}Ba + ^{96}Sr + ^{10}Be	8.30×10^{-4}	1.95×10^{-16}	1.30×10^{-14}	1.43×10^{-14}	0.656
^{144}Ba + ^{98}Sr + ^{10}Be	4.60×10^{-3}	1.92×10^{-16}	5.05×10^{-14}		
^{142}Ba + ^{100}Sr + ^{10}Be	2.40×10^{-4}	1.39×10^{-16}	4.35×10^{-14}		
^{142}Xe + ^{100}Zr + ^{10}Be	2.70×10^{-2}	1.15×10^{-16}	2.13×10^{-15}		
^{140}Xe + ^{102}Zr + ^{10}Be	3.00×10^{-2}	6.98×10^{-17}	8.11×10^{-15}		
^{138}Xe + ^{104}Zr + ^{10}Be	8.60×10^{-3}	6.45×10^{-17}	2.15×10^{-15}		
^{136}Te + ^{106}Mo + ^{10}Be	5.40×10^{-2}	5.35×10^{-17}	1.98×10^{-15}		
^{134}Te + ^{108}Mo + ^{10}Be	3.20×10^{-3}	3.13×10^{-17}	1.30×10^{-13}		
^{132}Sn + ^{110}Ru + ^{10}Be	3.80×10^{-3}	3.22×10^{-17}	6.99×10^{-15}		
^{130}Sn + ^{112}Ru + ^{10}Be	1.50×10^{-2}	2.98×10^{-17}	3.60×10^{-14}		
^{140}Xe + ^{98}Sr + ^{14}C	3.50×10^{-3}	4.96×10^{-25}	1.84×10^{-22}	6.54×10^{-23}	0.505
^{138}Xe + ^{100}Sr + ^{14}C	4.40×10^{-4}	4.89×10^{-25}	1.22×10^{-23}		
^{136}Te + ^{102}Zr + ^{14}C	6.90×10^{-3}	2.85×10^{-25}	7.31×10^{-23}		
^{134}Te + ^{104}Zr + ^{14}C	3.90×10^{-3}	2.35×10^{-25}	3.41×10^{-23}		
^{132}Sn + ^{106}Mo + ^{14}C	4.00×10^{-2}	1.08×10^{-25}	2.45×10^{-22}		
^{130}Sn + ^{108}Mo + ^{14}C	2.70×10^{-3}	9.98×10^{-26}	2.85×10^{-23}		

yields, for the investigated channels, are listed in the third and fourth columns of Table II, respectively. While the values of (S_6He) based on the calculated yields at $E_I^* = 3$ MeV lies between 5.1×10^{-6} and 3.1×10^{-3} with an average value of 4.6×10^{-4}, that estimated with $E_I^* = 4$ MeV ranges between 6.3×10^{-7} and 5.2×10^{-4} with an average value of 7.5×10^{-5}. These values of E_I^* are the optimum excitation energy of the similar heaviest nuclei participating in the ^{4}He channels.

Also, 10 and 14 ternary fragmentation channels of ^{252}Cf were observed with ^{10}Be and ^{14}C, respectively, as emitted light particles. These channels and their relative yields are given in Table II. No new heavy nuclei were observed either as A_1 or A_2 nuclei unlike those observed in the ^{4,6}He channels. The highest relative yields were observed for the ternary fragmentation channels of (^{136}Te, ^{106}Mo, ^{10}Be; $Y_{\rm exp} = 0.054\%$) and (^{132}Sn, ^{106}Mo, ^{14}C; 0.040%). The total relative yields for the ^{10}Be and ^{14}C channels are about 0.147% and 0.057%, respectively. The kinetic energy of the emitted ^{10}Be (^{14}C) cluster corresponding to the maximum indicated yield is about 18.8 MeV (26.0 MeV). Displayed in Figs. 5(a) and 5(b) are, respectively, the decimal logarithms of the ^{10}Be and ^{14}C preformation probabilities, as extracted from calculated yield $Y_{\rm cal}(E_I)$ and the experimental yield values $Y_{\rm exp}$. The yield calculations are performed within the range of $E_I^*(E_{A_1}^*, E_{A_{CN23}}^*) = 1$–7 MeV for the ^{10}Be and ^{14}C channels. The solid and dashed lines in Fig. 5 are drawn to guide the eye for the calculations performed at the different values of E_I^*. Figure 5 shows that the extracted preformation probability of ^{10}Be and ^{14}C inside between the two heavy nuclei inside the parent nucleus steadily decreases upon increasing the considered excitation energy of A_1. The average relative yields that calculated at excitation energies $E_I^* = 3$ and 4 MeV for the ^{10}Be and ^{14}C fragmentation channels and the corresponding average preformation probabilities as extracted from these calculations along with the experimental values are listed in Table II. While the values of $S_{^{10}\rm Be}$ that estimated from the calculated yields at $E_I^* = 3$ MeV ranges between 3.5×10^{-15} and 2.3×10^{-13}

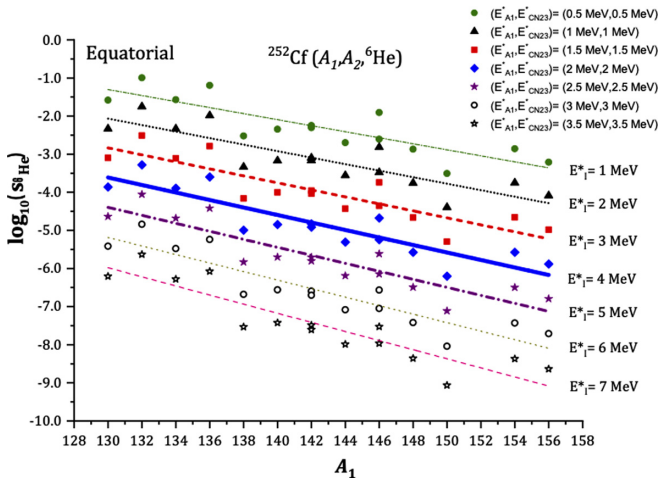

FIG. 4. Logarithms of the ^{6}He preformation probability [$\log_{10}(S_6\text{He})$] versus A_1 for the observed ^{6}He ternary fission channels of ^{252}Cf, extracted from Y_{exp} and Y_{cal} (E^*_I = 1–7 MeV) and considering equatorial configuration of the fragments. The solid and dashed lines are drawn to guide the eye.

with an average value of 5.1×10^{-14}, that estimated at $E^*_I = 4$ MeV lies between 4.7×10^{-16} and 3.0×10^{-14} with an average value of 7.5×10^{-15}. On the other hand, the values of $S_{^{14}C}$ estimated from the yields at $E^*_I = 3$ MeV ranges between 2.1×10^{-23} and 4.3×10^{-22} with an average value of 1.7×10^{-22}, while the estimated values at $E^*_I = 4$ MeV lie between 3.6×10^{-24} and 6.3×10^{-23} with an average value of 2.1×10^{-23}. The results presented in Fig. 5 and Table II indicate that the preformation probability of the emitted light particle sharply decreases with increasing its mass number.

Drawn in Fig. 6 are the estimated average preformation probability, as a function of the mass number A_3, as extracted from the calculations performed at $E^*_I(E^*_{A_1}, E^*_{A_{CN23}})$ = 2–5 MeV for the different ternary fission channels presented in Tables I and II. Figure 6 shows that $S_c(A_3)$ exponentially decreases as a function of A_3. A less decreasing trend of $S_c(A_3)$ with E^*_I is shown in Fig. 6. The average value of $S_c(A_3)$ that obtained considering the different channels at the optimum excitation energies of $E^*_I = 3$ and 4 MeV can be fitted as a function of A_3 as

$$S_c = 10^7 e^{-4.8A_3}. \tag{18}$$

The open circles in Fig. 6 represent the preformation probability when it is calculated using the phenomenological formula given by Eq. (18). The dimensionless coefficient −4.8 in the exponent of formula (18) represents the exponential decay constant of the preformation probability (S_{A_3}), as a function of A_3. The standard deviations of the average estimated values of S_{A_3} ($E^*_I = 3$ and 4 MeV) for the different observed ^{4,6}He, ^{10}Be, and ^{14}C ternary fission channels of ^{252}Cf relative to the values estimated by Eq. (18) are 0.752, 1.553, 0.656, and 0.505, respectively.

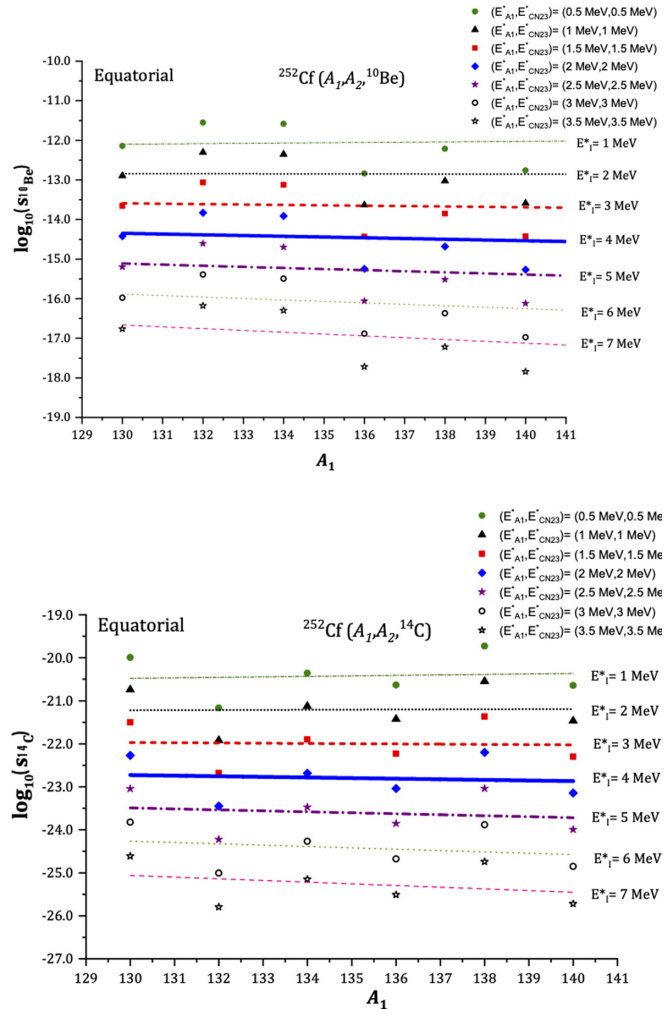

FIG. 5. Same as in Fig. 4 but for the (a) ^{10}Be and (b) ^{14}C ternary fission channels of ^{252}Cf.

IV. CONCLUSIONS

We have used the equatorial tripartition kinematics to probe the preformation probability of the light nucleus emitted in the ^{4,6}He, ^{10}Be, and ^{14}C ternary fission channels of the ^{252}Cf. The lightest nucleus is probably clustered as a recognized entity, with a certain preformation probability, in the neck region joining the binary fissioning system composed of the heaviest produced nucleus and the intermediate nucleus of $A_2 + A_3$. The preformation probability has been estimated by comparing the calculated relative yield to the experimentally observed yield. The calculations have shown that the optimum excitation energy of heaviest nucleus involved in the ternary fission process that includes an α particle is ranged between 3 MeV and 4 MeV. The estimated α-preformation probability in such ternary fission channels lies in the range of 10^{-1}–10^{-3}. This range is comparable with that estimated for the α decays of the medium mass nuclei neighboring to the intermediate nuclei involved in the investigated ternary fission channels. Increasing the excitation energy E^*_I is found to decrease the calculated relative yields, and consequently indicate less preformation probability. Increasing the value of the excitation

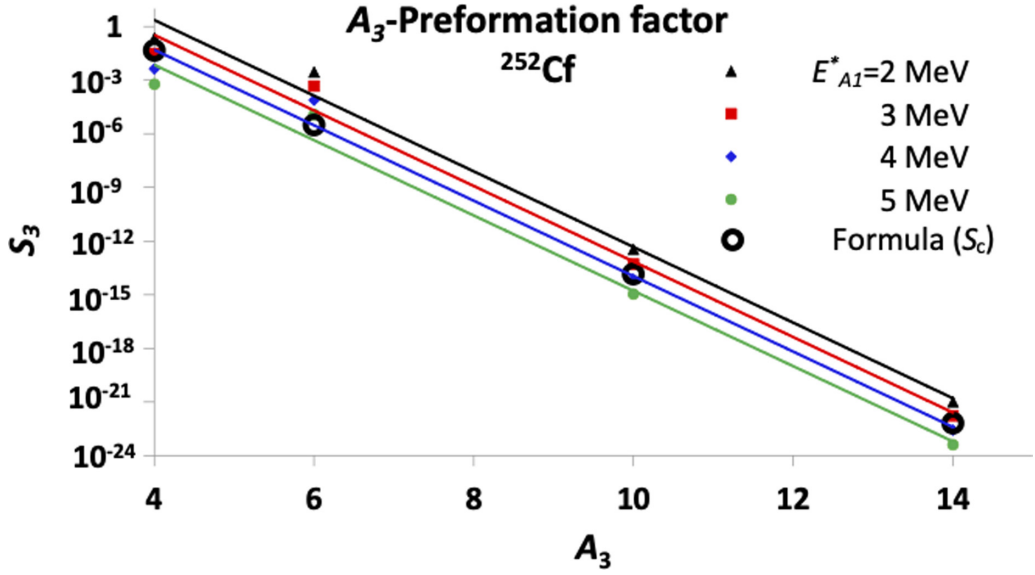

FIG. 6. Estimated average preformation probability against the mass number of the light emitted nucleus A_3, as extracted from the calculations performed at $E^*_I(E^*_{A_1}, E^*_{A_{CN23}}) = 2$–5 MeV for the different ^{4,6}He, ^{10}Be, and ^{14}C ternary fission channels of ^{252}Cf (presented in Tables I and II). The open circles represent the values of the preformation probability given by [S_c: Eq. (18)].

energy of the prior stage (I) by about 1 MeV decreases the order of magnitude of the estimated average value of preformation probability by about one order of magnitude. The calculations based on excitation energies smaller than 2 MeV yielded unphysical large values of the preformation probability. The preformation probability of the emitted light particles heavier than ^{4}He exponentially decreases with increasing its mass number. Based on the obtained results, a phenomenological formula is suggested to give the preformation probability of a given emitted cluster as a function of its mass number A_3. This formula would help in predicting and investigating the probable ternary fission channels of heavy and superheavy nuclei.

ACKNOWLEDGMENTS

This work is supported by the Egyptian Academy of Scientific Research And Technology (ASRT), Science-Up Grant ID 6588.

[1] D. N. Poenaru, W. Greiner, J. H. Hamilton, A. V. Ramayya, E. Hourany, and R. A. Gherghescu, Phys. Rev. C **59**, 3457 (1999).
[2] D. N. Poenaru, B. Dobrescu, W. Greiner, J. H. Hamilton, and A. V. Ramayya, J. Phys. G: Nucl. Part. Phys. **26**, L97 (2000).
[3] V. I. Zagrebaev, A. V. Karpov, and W. Greiner, Phys. Rev. C **81**, 044608 (2010).
[4] Y. V. Pyatkov *et al.*, Rom. Rep. Phys **59**, 569 (2007).
[5] Y. V. Pyatkov *et al.*, Eur. Phys. J. A **45**, 29 (2010).
[6] Y. V. Pyatkov *et al.*, Eur. Phys. J. A **48**, 94 (2012).
[7] A. K. Nasirov, W. von Oertzen, A. I. Muminov, and R. B. Tashkhodjaev, Phys. Scr. **89**, 054022 (2014).
[8] W. von Oertzen, A. K. Nasirov, and R. B. Tashkhodjaev, Phys. Lett. B **746**, 223 (2015).
[9] W. Von Oertzen, Y. V. Pyatkov, and D. Kamanin, Acta. Phys. Pol. B **44**, 447 (2013).
[10] K. P. Santhosh and S. Krishnan, Eur. Phys. J. A **52**, 108 (2016).
[11] K. Manimaran and M. Balasubramaniam, Phys. Rev. C **83**, 034609 (2011).
[12] K. P. Santhosh, S. Krishnan, and B. Priyanka, Int. J. Mod. Phys. E **23**, 1450071 (2014).
[13] J. H. Hamilton *et al.*, Prog. Part. Nucl. Phys **38**, 273 (1997).
[14] A. V. Ramayya *et al.*, Prog. Part. Nucl. Phys. **46**, 221 (2001).
[15] A. V. Daniel, G. M. Ter-Akopian, J. H. Hamilton, A. V. Ramayya, J. Kormicki, G. S. Popeko, A. S. Fomichev, A. M. Rodin, Y. T. Oganessian, J. D. Cole, J. K. Hwang, Y. X. Luo, D. Fong, P. Gore, M. Jandel, J. Kliman, L. Krupa, J. O. Rasmussen, S. C. Wu, I. Y. Lee, M. A. Stoyer, R. Donangelo, and W. Greiner, Phys. Rev. C **69**, 041305(R) (2004).
[16] A. V. Ramayya *et al.*, Phys. Rev. C **57**, 2370 (1998).
[17] A. V. Ramayya, J. H. Hamilton, and J. K. Hwang, Rom. Rep. OF Phys. **59**, 595 (2007).
[18] C. Wagemans, *The Nuclear Fission Process* (CRC Press, Boca Raton, FL, 1991).
[19] S. Vermote, C. Wagemans, O. Serot, J. Heyse, J. Van Gils, T. Soldner, and P. Geltenbort, Nucl. Phys. A **806**, 1 (2008).
[20] A. V. Ramayya *et al.*, Phys. Rev. Lett **81**, 947 (1998).
[21] P. Singer, Y. N. Kopatch, M. Mutterer, M. Klemens, A. Hotzel, D. Schwalm, P. Thirolf, and M. Hesse, in *Proceedings of the Third International Conference on Dynamical Aspects of Nuclear Fission, Casta Papiernica, Slovakia*, edited by J. Kliman and B. Pustylink (Joint Institute for Nuclear Research, Dubna, 1996), p. 262.
[22] Y. N. Kopatch, M. Mutterer, D. Schwalm, P. Thirolf, and F. Gönnenwein, Phys. Rev. C **65**, 044614 (2002).

[23] M. Ismail, W. M. Seif, and A. S. Hashem, Eur. Phys. J. A **52**, 317 (2016).
[24] M. Ismail, W. M. Seif, A. S. Hashem, M. M. Botros, and I. A. M. Abdul-Magead, Ann. Phys. (NY) **372**, 375 (2016).
[25] M. R. Pahlavani, O. N. Ghodsi, and M. Zadehrafi, Phys. Rev. C **96**, 054612 (2017).
[26] K. P. Santhosh, S. Krishnan, and B. Priyanka, Eur. Phys. J. A **50**, 66 (2014).
[27] G. Alvarez Farwell, E. Segrè, and C. Wiegand, Phys. Rev **71**, 327 (1947).
[28] G. M. Ter-Akopian *et al.*, in *Proceedings of the Third International Conference on Fission and Properties of Neutron-Rich Nuclei* (World Scientific, Singapore, 2003), p. 535.
[29] C. M. Herbach *et al.*, Nucl. Phys. A **712**, 207 (2002).
[30] J. P. Theobald, P. Heeg, and M. Mutterer, Nucl. Phys. A **502**, 343 (1989).
[31] J. P. Theobald, Ph.D thesis, Institut für Kernphysik, Technische Hochschule, Darmstadt, FRG, 1985.
[32] A. Sandulescu, A. Florescu, F. Carstoiu, W. Greiner, J. H. Hamilton, A. V. Ramayya, and B. R. S. Babu, Phys. Rev. C **54**, 258 (1996).
[33] K. R. Vijayaraghavan, W. von Oertzen, and M. Balasubramaniam, Eur. Phys. J. A **48**, 27 (2012).
[34] P. Holmvall, U. Köster, A. Heinz, and T. Nilsson, Phys. Rev. C **95**, 014602 (2017).
[35] M. Csatlós *et al.*, Phys. Lett. B **615**, 175 (2005).
[36] A. Sandulescu, A. Florescu, F. Carstoiu, A. V. Ramayya, J. H. Hamilton, J. K. Hwang, B. Babu, and W. Greiner, Int. J. Mod. Phys. E **7**, 626 (1998).
[37] D. Vautherin and D. M. Brink, Phys. Rev. C **5**, 626 (1972).
[38] J. Bartel and K. Bencheikh, Eur. Phys. J. A **14**, 179 (2002).
[39] E. Chabanat, P. Bonche, P. Haensel, J. Meyer, and R. Schaeffer, Nucl. Phys. A **635**, 231 (1998).
[40] P. Bonche, H. Flocard, and P. H. Heenen, Nucl. Phys. A **467**, 115 (1987).
[41] F. l. Stancu and D. M. Brink, Nucl. Phys. A **270**, 236 (1976).
[42] J. C. Slater, Phys. Rev **81**, 385 (1951).
[43] C. Titin-Schnaider and P. H. Quentin, Phys. Lett. B **49**, 213 (1974).
[44] W. M. Seif and H. Mansour, Int. J. Mod. Phys. E **24**, 1550083 (2015).
[45] W. M. Seif and A. S. Hashem, Chin. Phys. C **42**, 064104 (2018).
[46] W. M. Seif, Phys. Rev. C **91**, 014322 (2015).
[47] W. M. Seif, M. M. Botros, and A. I. Refaie, Phys. Rev. C **92**, 044302 (2015).
[48] J. J. Morehead, J. Math. Phys. **36**, 5431 (1995).
[49] B. Buck, A. C. Merchant, and S. M. Perez, Phys. Rev. Lett **72**, 1326 (1994).
[50] B. Buck, J. C. Johnston, A. C. Merchant, and S. M. Perez, Phys. Rev. C **53**, 2841 (1996).
[51] S. A. Gurvitz and G. Kalbermann, Phys. Rev. Lett **59**, 262 (1987).
[52] N. G. Kelkar and H. M. Castãneda, Phys. Rev. C **76**, 064605 (2007).
[53] NuDat2.7, Nuclear Structure and Decay Data, http://www.nndc.bnl.gov/nudat2/.
[54] G. Audi, F. G. Kondev, M. Wang, W. J. Huang, and S. Naimi, Chin. Phys. C **41**, 030001 (2017).